

Effects of arousal and movement on secondary somatosensory and visual thalamus

Gordon H. Petty^{1,2,3,5}, Amanda K. Kinnischtzke^{1,2,3,5}, Y. Kate Hong^{1,2,3,4}, and Randy M. Bruno^{1,2,3,*}

¹ Dept. of Neuroscience, Columbia University, New York, NY, 10027 USA

² Kavli Institute for Brain Science, Columbia University, New York, NY, 10027 USA

³ Zuckerman Mind Brain Behavior Institute, Columbia University, New York, NY, 10027 USA

⁴ Present Address: Department of Biological Sciences and Carnegie Mellon Neuroscience Institute, Carnegie Mellon University, Pittsburgh, PA 15206 USA

⁵ These authors contributed equally

* Correspondence: randybruno@columbia.edu (R.M.B.)

1 **Abstract**

2 All neocortical sensory areas have an associated primary and secondary thalamic nucleus. While the
3 primary nuclei encode sensory information for transmission to cortex, the nature of information
4 encoded in secondary nuclei is poorly understood. We recorded juxtасomally from neurons in
5 secondary somatosensory (POm) and visual (LP) thalamic nuclei of awake head-fixed mice with
6 simultaneous whisker tracking and pupilometry. POm activity correlated with whether or not a mouse
7 was whisking, but not precise whisking kinematics. This coarse movement modulation persisted after
8 unilateral paralysis of the whisker pad and thus was not due to sensory reafference. POm continued
9 to track whisking even during optogenetic silencing of primary somatosensory and motor cortex and
10 after lesion of superior colliculus, indicating that motor efference copy cannot explain the correlation
11 between movement and POm activity. Whisking and pupil dilation were strongly correlated, raising the
12 possibility that POm may track arousal rather than movement. LP, being part of the visual system, is
13 not expected to encode whisker movement. We discovered, however, that LP and POm track whisking
14 equally well, suggesting a global effect of arousal on both nuclei. We conclude that secondary
15 thalamus is a monitor of behavioral state, rather than movement, and may exist to alter cortical activity
16 accordingly.

17

18 **Main**

19 Somatosensory, visual, auditory, and gustatory cortex are each reciprocally connected with a specific
20 subset of thalamic nuclei. These nuclei can be subdivided into primary and secondary (often termed
21 “higher-order”) nuclei¹⁻³. The primary nuclei are the main source of sensory input to the cortex and
22 respond robustly to sensory stimulation with low latency⁴⁻⁷. Unlike primary nuclei, the secondary nuclei
23 are interconnected with many cortical and subcortical regions, and their role in sensation and cognition
24 is poorly understood.

25 In rodents, the facial whisker representation of primary somatosensory cortex (S1) is tightly integrated
26 with two thalamic nuclei: the ventral posteromedial nucleus (VPM) and the posterior medial nucleus
27 (POm). Compared to the primary nucleus VPM, the secondary nucleus POm has broader receptive
28 fields, longer-latency sensory responses, and poorly encodes fine aspects of whisker touch such as
29 contact timing and stimulus frequency⁸⁻¹¹. It receives input from S1, motor cortex, posterior parietal
30 cortex, the zona incerta, and many other subcortical regions in addition to brainstem afferents^{4,12,13}.
31 Whereas VPM innervates cortical layer 4 and the border of layers 5B and 6, POm projects to the apical
32 dendrites of layer 1 as well as layer 5A⁶. POm is a stronger driver of layer 2/3 cells than cortico-cortical
33 synapses and can enhance sensory responses in pyramidal neurons of layers 2/3 and 5^{14,15}. POm is
34 thus positioned to strongly influence sensory computations in S1 and do so in ways that are highly
35 distinct from VPM. However, what POm activity encodes remains a mystery.

36 One possibility is that POm activity encodes self-generated movements, through either sensory
37 reafference (stimulation of the sensory receptors by active movement) or motor efference copy
38 (internal copies of motor commands), rather than extrinsic tactile sensations¹⁶. If secondary thalamus
39 were a monitor of movements⁵, somatosensory cortex could use POm input to differentiate self-
40 generated and externally generated sensory signals. However, recent studies in awake animals have
41 observed that, in comparison to VPM, POm poorly encodes whisker motion and contact^{8,17}, which
42 casts doubt on the hypothesis that secondary pathways provide detailed motor information to cortex.

43 An alternative hypothesis is that secondary thalamus is a key structure for monitoring behavioral state.
44 For instance, several studies have noted that a subset of POm neurons are activated by pain^{18,19}, a
45 powerful stimulus that can trigger a change in animal’s state. Spatial attention is a more subtle form

46 of behavioral state change and has been implicated repeatedly in studies of primate secondary visual
47 thalamus (lateral pulvinar)^{20–22}. The rodent homolog to the pulvinar (lateral posterior nucleus, LP) is
48 active during mismatch of movement and visual stimuli²³, which might reflect elevations in visual
49 attention or even global arousal. These results raise the possibility that modulation by behavioral state
50 is a general feature of all secondary nuclei.

51 Here we investigate how afferent, corticothalamic, and collicular inputs— the three main excitatory
52 pathways to secondary sensory thalamus— influence encoding of movements by POM in the awake
53 mouse. We discovered that removing these circuits enhances rather than reduces modulation of POM
54 activity by movements, suggesting that these pathways may mainly transmit signals of a nature other
55 than movement. We further examine how POM activity compares to that of LP - which have not been
56 directly compared before - to investigate general principles of secondary thalamus function. This
57 comparison reveals that behavioral state, rather than movement itself, prominently dictates the activity
58 of secondary thalamus.

59

60 Results

61 We characterized the degree to which POM encodes whether or not an animal is whisking versus the
62 fine details of whisking movements. We recorded juxtасomally from single neurons in head-fixed mice
63 while acquiring high-speed video of the contralateral whisker field, from which whisker positions could
64 be algorithmically extracted (Figure 1a, b)²⁴. To measure slow aspects of whisking, we calculated
65 whisking amplitude from the median angle of all whiskers. Whisking amplitude is defined as the
66 difference in angle between minimum and maximum protraction over the whisking cycle (Hill *et al.*,
67 2011; Moore *et al.*, 2015, see Methods). Whisking amplitude was then used to determine periods of
68 quiescence and whisking, as defined by periods of time when whisking amplitude exceeded 20% of
69 the maximum for more than 250 msec (Figure 1b, shaded areas).

70 Whisking substantially elevated POM firing rates. We computed the mean firing rate for each cell
71 during periods when the mouse was whisking versus quiescent (Figure 1c, 22 POM neurons in 5
72 mice). The firing rates of POM cells were significantly higher during bouts of whisking, increasing from
73 a mean firing rate of 7.8Hz to 12.4 Hz (58.5% increase, $p < 10^{-4}$, paired t-test). To understand which
74 components of whisking might drive POM activity, we calculated the cross-correlation between POM
75 firing rate and three features of whisking activity: the median angle (Figure 1d, gray), the amplitude
76 metric which captures the slow envelope of whisking (green), and the median angle bandpass-filtered
77 from 4-30 Hz (black), which reflects fast protractions and retractions of the whisker. We found that
78 POM neurons had little correlation with the bandpass-filtered angle, but prominent correlations with
79 both whisker angle and whisking amplitude around a time lag of zero. The strongest correlate of POM
80 activity was whisking amplitude, suggesting that POM is coupled to the slow components of whisking,
81 rather than tracking individual whisk cycles.

82 To further investigate the encoding of the fast components of whisking in POM, we analyzed whether
83 individual cells preferred to discharge during a certain phase of the whisking bout. We quantified the
84 phase of whisking by applying the Hilbert transform to the bandpass-filtered median whisker. We
85 identified the phase at which each action potential occurred during whisking and plotted distributions
86 of firing rate as a function of phase. For each cell, we fit a sinusoid to characterize the cell's preferred
87 phases (the phase of the whisk cycle that elicited the highest firing rate) and modulation depth (the
88 degree to which phase impacts firing rate, measured as the peak-trough difference normalized by
89 mean firing rate). Figure 1e shows the phase relationship of two example cells: one with significant
90 coding (top) and the other insignificant (bottom). Most POM cells (17/22) resembled the non-phase
91 coding example, having little or no modulation (right). Together, these results indicate that the majority

92 of POM cells do not encode fast whisking dynamics such as whisker angle or the phase of the whisking
93 cycle. Rather, they track overall whisking activity, *i.e.* the whisking versus quiescence.

94 One possible source of whisking-related activity is refferent sensory input: when the mouse whisks,
95 the self-generated movement could deform the whisker follicle and stimulate mechanoreceptors. To
96 measure the degree to which POM activity is driven by the sensory refference caused by whisking,
97 we severed the facial motor nerve on the right side of the face (Figure 2a), contralateral to our
98 recordings, while taking video of the left (ipsilateral) side of the face. This manipulation does not
99 damage the sensory neurons and avoids the risk of inducing sensory neuron plasticity (Shetty,
100 Simons, 2003). Mice were no longer able to move the right whisker pad, but the whisking on the left
101 side of the face was unaffected (Figure 2b). Without whisker movement, there can be no refferent
102 sensory input from the right whisker pad. As in intact mice, firing rates of POM neurons in nerve cut
103 animals were significantly higher during whisking bouts (Figure 2c, $n = 12$, $p = 0.0007$, paired t test)
104 and to a similar degree, increasing from quiescent firing rate of 11.6Hz to a whisking rate of 16.7Hz
105 (44%). POM firing rates also correlated with ipsilateral whisking amplitude, at a similar magnitude and
106 with a similar lag as in the contralateral whisker field in intact mice (Figure 2d). This demonstrates that
107 the correlation of POM activity and overall whisking is not due to ascending refferent information.

108 We also calculated the phase coding of the ipsilateral whisker field (Figure 2e) and compared it to
109 phase coding of the contralateral whisker field (Figure 1e). While average modulation depth was
110 unchanged (Figure 2e $p = 0.12$, Wilcoxon rank-sum test), modulation depth by definition is
111 bounded at zero, complicating analysis of medians close to zero. Indeed, there was a noticeable and
112 statistically significant decrease in the range of modulation depths in the transected group (Figure 2f,
113 $p = 0.0013$, two-sample F-test), consistent with nerve cut eliminating the largest modulation values.
114 These results suggest that refferent signals do not contribute to changes in POM activity reflecting
115 the slow envelope of whisking (Figure 2d) but are responsible for the small population of POM cells
116 carrying fast phase information (Figure 2e).

117 POM is reciprocally connected to several cortical areas, potentially making cortical input a strong driver
118 of POM activity^{4,15,26}. In particular, input from S1 and primary motor cortex (M1) could convey
119 sensorimotor information, such as a motor efference copy, that would drive whisking-related activity,
120 independent of ascending sensory input. To test this, we expressed halorhodopsin in all excitatory
121 cortical neurons by crossing Emx1-Cre mice with a conditional halorhodopsin responder line, a
122 technique we previously used to silence S1²⁷. We recorded from POM cells while silencing S1 or M1
123 with an amber laser (Figure 3a). Here, we were similarly able to inhibit M1 activity (Figure 3b).

124 M1 suppression reduced the baseline firing rate of POM cells, but POM activity was still elevated
125 during whisking regardless of whether the laser was on or off (Figure 3c). Suppressing M1 increased
126 the correlation between POM firing rate and whisking amplitude (Figure 3d). This suggests that POM
127 encoding of fine whisking kinematics arises from ascending sensory refference rather than input from
128 motor cortex.

129 To confirm that these effects were due to inhibition of M1 inputs to POM and not an artifact of
130 optogenetic-induced changes in whisking behavior, we also recorded from cells in VPM. VPM, which
131 does not receive direct projections from M1, was largely unaffected by M1 inhibition. We observed no
132 effect of inhibition on VPM firing rates or cross-correlation between VPM activity and whisking (Figure
133 3e, f).

134 In a parallel set of experiments, we silenced S1 using the same cre-dependent halorhodopsin line
135 (Figure 4a). We recently demonstrated that this technique robustly blocks action potentials throughout
136 all cortical layers of S1 in awake behaving mice²⁷. Silencing S1 reduced POM activity whether mice
137 were whisking or quiescent (Figure 4b), $n = 11$ cells, 3 mice; whisking $p = 0.0002$, laser $p = 0.024$,

138 two-way repeated measures ANOVA). As in the M1 experiments, the correlation between whisking
139 amplitude and POm activity was, if anything, unchanged or increased by S1 silencing (Figure 4c, laser-
140 off peak correlation = 0.036, laser-on peak correlation = 0.081. There was a tendency for S1 inhibition
141 to reduce overall activity in VPM, possibly reflecting the known corticothalamic connections between
142 S1 and VPM^{28–30}, but this effect did not reach significance (Figure 4d; $p = 0.1$). Suppressing S1 had
143 little impact on the correlation of VPM spiking and whisking (Figure 4e), though there was a trend for
144 S1 inhibition to increase modulation depth (increase from 0.17 to 0.32, 91% change, $p = 0.057$).

145 Thus, both optogenetic manipulations had qualitatively different effects on VPM and POm activity,
146 consistent with the known anatomical differences in corticothalamic projections onto these two nuclei.
147 Together, these results demonstrate that POm does not inherit information about whisking amplitude
148 from M1 or S1. Rather, corticothalamic inputs appear to transmit signals other than whisker
149 movements, and these additional signals reduce the correlation of POm activity with whisking
150 amplitude and phase.

151 In addition to afferent inputs from brainstem and efferent inputs from cortex, POm receives excitatory
152 projections from the superior colliculus (SC)³¹, which could also provide a motor efference copy signal
153 similar to known collicular circuits in the visual system³². SC receives excitatory input from both the
154 trigeminal brainstem³³ as well as cortex, making SC a potential source of whisking-related POm
155 activity. To test this possibility, we performed bilateral electrolytic lesions in SC and subsequently
156 recorded POm cells (Figure 5a). Whisking had similar effects on POm activity in both intact and
157 lesioned animals (Figure 5b, $n = 49$ cells from 8 animals, 59% increase in mean firing rate, $p < 10^{-9}$).
158 POm firing rates of lesioned mice were overall higher than those of intact animals, independent of
159 whether animals were whisking or quiescent (Figure 5c, lesion $p < 10^{-3}$, whisking $p < 10^{-5}$, 2-way
160 ANOVA). There was a slight tendency for SC-lesioned animals to whisk more frequently than intact
161 animals, but this effect was not statistically significant (Figure 5d, $p = 0.35$, Wilcoxon rank-sum test).
162 We conclude that SC is not responsible for the whisking-induced elevation of POm activity.

163 Neither reafference nor the most likely sources of motor efference copy explain the coarse modulation
164 of POm by movement. This raises the question of whether POm encodes movement *per se*, or another
165 variable that is coupled with whisking and other movements, such as arousal. To investigate this, we
166 measured pupil diameter, which is a known metric of arousal. We acquired videos of the pupil and
167 whiskers while recording from POm (Figure 6a). Pupil diameter was tightly correlated with whisking,
168 with pupil dilation lagging whisking amplitude by 880 msec on average (Figure 6b). Pupil diameter also
169 correlated with POm activity, to a similar degree as whisking and with a lag of 950 msec (Figure 6c,
170 whisking amplitude peak correlation = 0.052, pupil diameter peak correlation = 0.071, $p = 0.23$, paired
171 t-test).

172 We reasoned that, if the modulation of POm by whisking was truly due to whisker movement rather
173 than some other correlated variable, non-somatosensory thalamic nuclei would not be expected to
174 track whisking. The secondary visual thalamic nucleus LP is the rodent homolog of the primate lateral
175 pulvinar. LP is primarily coupled with cortical and subcortical visual areas³⁴, rather than somatosensory
176 ones. Because of their different connectivity, POm and LP are expected to carry separate sensorimotor
177 signals related to somatosensation and vision, respectively. Therefore, LP would not be expected to
178 encode whisker movement. By contrast, changes in behavioral state, such as overall animal arousal
179 as suggested by our pupil measurements, might modulate all thalamic nuclei, including LP and POm.

180 We tested this idea by recording juxtасomally from LP neurons (Figure 7a, b; 29 cells from 4 mice).
181 Surprisingly, we found that LP activity was significantly increased during whisking bouts (Figure 7c,
182 increase from 13.0Hz to 18.0Hz, $p < 10^{-4}$, paired t test). Like POm, LP activity correlated with both
183 whisking amplitude and median whisker angle with low latency (Figure 7d). Since changes in pupil

184 diameter will cause more light to fall on the retina, the LP correlation with whisking might be an artifact
185 of pupil dilation. To control for this, a subset of cells were recorded in low light. Under these darker
186 conditions, the pupil was maximally dilated and did not change (Figure 7b), rendering input to the
187 retina largely constant. However, these cells still showed an equivalent increase in firing rate during
188 whisking (Figure 7c, orange; $n = 29$ cells, 4 animals; increase from a mean of 13.0Hz to 18.0 Hz, or
189 39%, $p < 10^{-4}$, paired t-test). Thus, LP activity appears to track whisking independent of changes in
190 visual input, which suggests that the effect in both nuclei is due to the arousal-whisking correlation
191 rather than a direct effect of whisking.

192 Together, our results indicate that the slow component of whisking-related activity in POm is neither a
193 consequence of ascending motion signals from reafferent mechanisms nor corticothalamic or
194 colliculothalamic efferent mechanisms. We conclude instead that behavioral state, such as arousal,
195 may strongly dictate the activity of secondary thalamic nuclei, including POm and LP.

196

197 Discussion

198 Our study tested the idea that secondary somatosensory thalamus is a monitor of movements or motor
199 commands and manipulated the multiple known pathways to POm that could mediate such signals.
200 Juxtosomal recordings of POm cells revealed that this nucleus mainly tracks slow components of
201 whisking, not detailed kinematics. Consistent with other studies^{8,17}, mouse POm firing rates are much
202 higher during bouts of whisking than when a mouse is quiescent. However, POm activity mainly
203 correlates with the slow change in whisking amplitude rather than the fast changes of the whisk cycle.
204 Only a minority of our POm cells exhibited any whisking phase information, and phase encoding
205 appeared to depend on sensory reafference. We have demonstrated that, by contrast, the overall
206 elevation of POm activity by whisking is not due to sensory reafference from self-generated
207 movements, as transection of the facial motor nerve did not uncouple POm activity from ipsilateral
208 whisking. We showed that potential motor efference copy via corticothalamic pathways from S1 and
209 M1 cannot account for whisking modulation of POm. Similarly, the phenomenon is independent of
210 superior colliculus, the activity of which is linked to movement and orienting.

211 What appears to be movement-related activity in POm is likely instead a consequence of the encoding
212 of behavioral state. Activity in secondary visual thalamus (LP) exhibits the same correlation with
213 whisker movement that we observed in POm. Though it is possible that POm and LP separately
214 encode correlated sensorimotor information, a more parsimonious explanation is that both POm and
215 LP are modulated by arousal, which is naturally elevated during movement. Modulation of activity by
216 behavioral state may be a general property of all secondary thalamic nuclei. Future studies are needed
217 to examine if this principle holds in auditory thalamic subnuclei and perhaps even thalamic nuclei
218 connected to motor cortex and other frontal areas. Conceivably, some movement correlations seen
219 even in motor thalamus³⁵ may reflect various states more than specific movements.

220 The paralemniscal system has been speculated to be a parallel secondary afferent pathway^{16,19}.
221 However, in anesthetized rats, POm does not appear to be sensitive to fine aspects of whisker touch,
222 having very large receptive fields and long-latency responses^{9,13}. One might expect that very large
223 synchronized movements of the whiskers, such as during whisking, would elicit a response from POm
224 due to sensory reafference driving coarse receptive fields. However, paralyzing the face did not
225 uncouple POm activity from ipsilateral whisking amplitude (Figure 2). Similarly, mouse barrel cortex is
226 also modulated by whisking and quiescence in absence of sensory input: whisking is associated with
227 a decrease in synchrony between layer 2/3 pyramidal cells in S1 and an increase in discharges by
228 VPM, which is unaltered by bilateral transection of the infraorbital nerve sensory nerve³⁶.
229 Manipulations of somatosensory thalamus strongly impacted cortical synchronization³⁷. Further

230 studies are needed to parcel out the extent to which thalamic contributions to cortical synchronization
231 is due to inputs from VPM, POM, or both.

232 POM receives descending input from many cortical regions including M1 and S1. Conceivably these
233 inputs could modulate ascending sensory input or provide the thalamus with a motor efference
234 copy^{15,38}. Similarly, LP and LGN axons in V1 exhibit eye movement-related signals²³. Previous studies
235 in anesthetized rats have shown that cortical inactivation will silence POM, but not VPM⁹. Therefore,
236 cortex might be the primary source of excitatory input to POM. However, we discovered that, in the
237 awake mouse, silencing either M1 or S1 only slightly reduces the firing rate of POM cells and has little
238 to no effect on VPM activity (Figure 3). We conclude that, while S1 and M1 provide significant
239 excitatory inputs to POM, these inputs are not the sole drivers of POM activity during wakefulness.

240 Moreover, silencing these corticothalamic pathways increased rather than decreased the correlation
241 between POM activity and whisking amplitude. If POM activity were primarily representative of a
242 cortical efference copy, we would expect the opposite effect. While we cannot rule out the possibility
243 that POM receives some efference copy from cortex, such input is not the cause of what at first
244 appears to be whisking modulation. POM might instead be under equal or greater control of subcortical
245 regions such as trigeminal brainstem complex, zona incerta, the thalamic reticular nucleus, and
246 neuromodulatory brainstem centers – all of which receive inputs from broad areas of the nervous
247 system^{13,39}.

248 As POM continues to track whisking in absence of both ascending sensory input and descending
249 cortical input, we propose that the activity we observe is not sensorimotor in nature, but rather
250 representative of thalamic coding of internal state. POM axons project to the apical dendrites of
251 pyramidal cells^{6,40}, where they might drive state-dependent changes in activity and synchrony. Arousal
252 has dramatic effects on cortical dynamics^{41–43}. We observed that pupil diameter, which closely tracks
253 arousal, is highly correlated with whisking amplitude. Due to the coupling between pupil and whisking
254 dynamics, they both correlate with POM firing rates (Figure 6). To dissociate the contributions of
255 arousal and whisker movement, we took the novel approach of comparing POM dynamics with those
256 of LP, the rodent homolog of the primate lateral pulvinar. We found a near-identical relationship
257 between LP activity and whisking as we observed in POM (Figure 7), even though there is no known
258 connectivity between LP and the whisker system. As for POM, these shifts in LP activity do not appear
259 to be sensory dependent, as they persist even in low-light conditions where the pupil is maximally
260 dilated and can no longer contribute to changes in retinal activity.

261 If state-dependent modulation of secondary thalamic nuclei is not derived from sensory reafference or
262 motor efference copy from cortex or superior colliculus, the likely remaining candidates would include
263 a large number of neuromodulators. For instance, zona incerta terminals within POM are regulated by
264 acetylcholine⁴⁴ and are likely modulated in the same way within LP. However, acetylcholine and
265 norepinephrine both track pupil dynamics⁴⁵, and both are also plausible mechanisms. In addition to
266 these two well-studied modulators, there are many others known to have functions in thalamus⁴⁶.
267 Furthermore, any of these modulators could act directly on POM and LP or indirectly through ZI, TRN,
268 brainstem nuclei, or other inputs.

269 The arousal effect we have described may be a more general version of modality-specific attentional
270 effects that have been proposed for at least some secondary thalamic nuclei. In primates, pulvinar
271 neurons respond strongest when stimuli are presented in attended regions of visual space⁴⁷, and
272 lesion of the pulvinar leads to deficits of selective attention during visual tasks^{22,48}. Human patients
273 with pulvinar damage exhibit spatial neglect, in which a stimulus can be perceived normally in isolation
274 but is missed or distorted in the presence of neighboring stimuli^{49,50}. By analogy, one might
275 hypothesize that POM provides feedback that selects somatosensory stimuli for further cortical

276 processing. Indeed, we and others have already demonstrated that activation of POm sensitizes
277 cortical pyramidal neurons to the occurrence of subsequent tactile stimuli^{14,15}. Thus, POm affords
278 control over the gain of the sensory responsiveness of somatosensory cortex circuitry. Selective
279 enhancement of sensory responses by attention within a modality could be a general principle of all
280 secondary thalamic function.

281 Cortex-wide fluctuations in activity are known to correlate with various uninstructed movements⁵¹
282 Cortical activity ceases in the absence of thalamic input^{35,52}, and secondary thalamic inputs to
283 somatosensory cortex are stronger and longer lasting than corticocortical connections¹⁴. Taking those
284 studies and our study together suggests that secondary thalamus may be the underlying cause of the
285 recently observed patterned fluctuations in activity across cortex. Our study directly tested the multiple
286 known possible sources of afferent and efferent motor signals to secondary thalamus. None of these
287 could explain apparent shifts in thalamic activity. Thus, behavioral state, rather than uninstructed
288 movement, may be a primary driver of thalamic and cortical activity during movement.

289 Elevated firing rates in secondary thalamus due to arousal or attention could be useful for creating
290 periods of heightened cortical plasticity. Recent studies have shown that repetitive sensory stimuli
291 in anesthetized animals drives POm input to pyramidal neurons, which leads to enhancement of
292 future sensory responses in cortex⁵³. A potential mechanism of this is that disinhibition of apical
293 dendritic spikes leads to long-term potentiation of local recurrent synapses among cortical
294 pyramidal neurons⁵⁴. Furthermore, an *in vivo* study found that associative learning can also
295 potentiate long-range POm connections onto pyramidal neurons when subsequently measured
296 *in vitro*⁵⁵.

297 It is conceivable that the arousal modulation of secondary thalamus that we have described is
298 utilized by such processes. Our work opens avenues to examining potential links between
299 arousal, attention, and plasticity.

300

301

302 **Acknowledgments**

303 The authors thank C. Kellendonk, A. Das, C. Rodgers, S. Benezra and G. Pierce for comments on the
304 manuscript and D. Baughman, B.C. Pil, and L. Jordan for technical support. This work was supported
305 by NIH R01 NS094659, R01 NS069679, and T32 EY013933.

306 **Author Contributions**

307 Conceptualization: AKK and RMB; Investigation: AKK and GHP; Formal Analysis: AKK, GHP, and
308 RMB; Optogenetics Methodology, Resources, and Assistance: YKH; Writing: GHP and RMB.

309 **Declaration of Interests**

310 The authors declare no competing interests.

311

312

313

314 **Figure titles and legends**

315

316 **Figure 1. POm cells mainly track slow components of whisking activity.** (a) An example frame
317 from a video, captured at 125 FPS. Identified whiskers are highlighted in green, and whisker bases
318 are indicated by yellow circles. (b) Example traces of juxtosomal POm recording and whisking. The
319 median angle of all whiskers in each video frame (middle, gray) was used to calculate the whisking
320 amplitude (bottom, green). (c) Scatter plot of POm firing rates during whisking and quiescence (n = 22
321 POm cells, 5 mice, increase from mean of 7.8Hz to 12.4 Hz, or 58%, $p < 10^{-4}$, paired t-test). *Green*,
322 cell in 1b. (d) Cross-correlation of POm firing rate and whisking amplitude (green), angle (gray), and
323 4-30 Hz bandpass-filtered angle (black). Shading, SEM over cells. Cross-correlation is normalized
324 such that autocorrelations at zero lag equal one. (e) *Left*, Firing rate as a function of phase in the
325 whisking cycle for two example POm units. A sinusoid model (black) was fit to each cell to quantify
326 preferred phase (white markers) and modulation depth. *Right*, A polar plot of modulation depth (radius)
327 and preferred phase (angle) of each POm unit. *Filled circles*, cells with significant phase modulation
328 ($p < 0.05$, Kuiper test, Bonferroni corrected).

329 **Figure 2. POm encodes whisking activity in absence of reafferent sensory input.** (a) The buccal
330 branch of the facial motor nerve was severed unilaterally, preventing whisker motion on the right side
331 of the face. Adapted from Heaton *et al.*, 2014⁵⁶. (b) Example POm cell (top, black), ipsilateral (left side
332 of face) whiskers (bottom, blue), and contralateral whiskers (*bottom, gray*). Blue boxes: periods of
333 whisking as in Fig.1B. (c) Scatter plot of mean POm firing rate during whisking and quiescence. *Blue*,
334 example cell in B. Firing rates during whisking are significantly higher than quiescence (n = 12 cells
335 from 2 animals, quiescent mean: 11.6Hz, whisking mean: 16.7Hz, 44% change, $p = 0.0007$, paired t
336 test). (d) Cross-correlation of POm firing rate and ipsilateral whisking amplitude. (e) Polar plot of
337 modulation depth and preferred phase of each POm unit as in Figure 1E. (f) Modulation depth of POm
338 cells in intact mice (green, as in Figure 1E) and after buccal nerve cut (blue). There was a significant
339 difference in the variance of modulation depth between groups ($p = 0.0013$, two-sample F test).

340 **Figure 3. Inhibition of primary motor cortex increases POm correlation with whisking.** (a)
341 Experimental setup. M1 was optogenetically silenced while recordings were made from M1, POm, or
342 VPM. Adapted from *The Mouse Brain Atlas in Stereotaxic Coordinates*⁵⁷. (b) Effect of laser on M1
343 activity (n = 26 M1 cells, 2 animals, mean decrease of 5.1 Hz, or 83%, $p = 0.0005$). (c) Individual (gray)
344 and mean (black or green) POm firing rates during whisking and quiescence when the laser is off or
345 on (n = 23 cells, 3 mice, whisking $p = 0.005$, laser $p = 0.016$, two-way repeated measures ANOVA).
346 (d) Cross-correlation of POm firing rate and whisking amplitude when the laser is off. The peak
347 correlation was significantly higher when the laser was on ($p = 0.0018$, paired t-test between peak
348 values). (e) Individual (gray) and mean (black or blue) VPM firing rates during whisking and quiescence
349 when the laser is off or on (n = 13 cells, 2 mice, whisking $p = 0.0002$, laser $p = 0.27$, two-way repeated
350 measures ANOVA). (f) Cross-correlation of VPM firing rate and whisking amplitude ($p = 0.11$, paired
351 t-test between peak values).

352 **Figure 4. Inhibition of primary somatosensory cortex increases POm correlation with whisking.**
353 (a) Experimental setup. (b) Individual (grey) and mean (black or green) POm firing rates during
354 whisking and quiescence when the laser is off or on. n = 11 cells, 3 mice, whisking $p = 0.0005$, laser
355 $p = 0.03$, two-way repeated measures ANOVA. (c) Cross-correlation between POm firing rate and
356 whisking amplitude when the laser is off (grey) or on (green). (d) Mean VPM firing rate (n = 8 cells, 2
357 mice. Whisking $p = 0.001$, laser $p = 0.11$, two-way repeated measures ANOVA). (e) Cross-correlation
358 between POm firing rate and whisking amplitude ($p = 0.057$, paired t-test between peak values).

359 **Figure 5. Lesions to superior colliculus do not reduce POM correlation with whisking. (a)**
360 Sample coronal section showing bilateral electrolytic lesion of superior colliculus. **(b)** Scatter plot of
361 POM firing rates during whisking and quiescence in lesioned (red) and intact animals (black, data from
362 Fig. 1). Firing rates in lesioned animals were significantly higher during whisking ($n = 49$ cells from 8
363 animals, increase from mean of 10.9Hz to 17.4Hz, or 59%, $p < 10^{-9}$, paired t-test). **(c)** Box plots of
364 POM firing rates during whisking (W) and quiescence (Q) in intact (black) and lesioned animals (red).
365 Pom firing rates in lesioned animals were higher than intact animals (whisking $p < 10^{-5}$, lesion $p < 10^{-3}$,
366 2-way ANOVA). **(d)** Lesioned animals tended to spend slightly more time whisking, but this was not
367 statistically significant (intact median = 27.5%, $n = 5$ mice; lesion median = 38.3%, $n = 8$ mice, $p =$
368 0.35, Wilcoxon rank-sum test).

369 **Figure 6. POM activity tracks pupil dynamics. (a)** Sample recording of POM activity (middle, black)
370 with concurrent ipsilateral pupil diameter (blue, top), median whisker angle (*middle, gray*), and
371 whisking amplitude (green, bottom). **(b)** Cross-correlation of pupil diameter and whisking amplitude
372 (30 recording sessions from 7 animals). Errors bars are present but very small. **(c)** Cross-correlation
373 of POM firing rate ($n = 10$ cells from 3 animals) with whisking amplitude (*green*) and pupil diameter
374 (*blue*).

375 **Figure 7. LP activity tracks slow whisker dynamics. (a,b)** Sample recordings of two LP cells (black)
376 recorded in normal light **(a)** or low light **(b)**, with corresponding median whisker angle (*gray*) whisking
377 amplitude (green), and pupil diameter (blue or orange). **(c)** Scatter plot of mean firing rate in LP cells
378 during whisking and quiescence. *Blue*, cells recorded in bright light; *Orange*, cells recorded in low light
379 ($p < 10^{-4}$, paired t-test). **(d)** Cross-correlation of LP firing rate with whisking amplitude (green), median
380 whisker angle (red), and 4-30 Hz bandpass filtered angle (black).

381

382

383

384

385

386

387

388

389

390 **Methods**

391 All experiments complied with the NIH Guide for the Care and Use of Laboratory Animals and were
392 approved by the Institutional Animal Care and Use Committee of Columbia University. Twenty-two
393 C57BL/6 mice were used in these experiments.

394 **Surgery**

395 Mice were anesthetized with isoflurane and placed in a stereotax. The skull was exposed, a thin layer
396 of superglue was applied, and a custom-cut stainless steel headplate was attached using dental
397 acrylic. A small (200 μm wide) opening was made on the mouse's left side at ~ 1.7 mm posterior to
398 bregma and 1.4 mm lateral of the midline. A silver wire or screw was inserted over the frontal cortex
399 of the same hemisphere as a ground electrode and covered with dental acrylic. The skin was sealed
400 to the implant using superglue. Mice were allowed to recover from surgery for 5 days before
401 habituation. Mice were habituated to the setup for 5 days by attaching their headplate to a holder on
402 the recording table for 5-30 min each day, during which no recordings were performed.

403 **Electrophysiology**

404 After habituation, a mouse would be recorded from for 3-7 days. A glass micropipette (opening ~ 1.5
405 μm ID, shank ~ 60 - 80 μm OD over last 3-4 mm) was filled with artificial cerebrospinal fluid (aCSF) and
406 inserted vertically into the brain using a micromanipulator. P_{OM} cells were typically recorded at
407 microdrive depths of 2800-3600 μm relative to the pia, and LP cells were recorded at depths of 2100-
408 2600 μm relative to pia. Recordings were made with a MultiClamp 700B amplifier (Molecular Devices),
409 bessel filtered 300-10,000 Hz, and digitized at 16 kHz using custom Labview software (ntrode). At the
410 end of some experiments, recording sites were labelled with a glass electrode coated in Dil inserted
411 to a depth of 3600 μm relative to the pia.

412 **Videography**

413 Whisker and pupil videos were made during electrophysiology and imaging using multiple PS3eye
414 cameras running at 125 frames per second. Camera housings had been removed, and the lenses
415 replaced with a 12 mm F2.0 lens (M12 Lenses Inc, part # PT-1220). Video was acquired using the
416 CodeLaboratories PS3eye camera driver and the GUVView software on linux computer.

417 **Optogenetics**

418 Optogenetic silencing of cortex was performed using Emx1-Halo mice as previously described²⁷.
419 Briefly, Emx1-IRES-Cre knock-in mice (Jackson Laboratories, stock #005628) were crossed to Rosa-
420 lox-stop-lox (RSL)-eNpHR3.0/eYFP mice (Ai39, JAX, stock# 006364), which express halorhodopsin
421 after excision of a stop cassette by Cre recombinase. All mouse lines were maintained on a C57BL/6
422 background. Optogenetic experiments used mice that were heterozygous for the desired transgene
423 as assessed by in-house genotyping. The locations of S1 and M1 were marked based on stereotaxic
424 coordinates during headplate surgery, and the skull was thinned before recordings. Light was
425 generated by a 593- or 594-nm laser (OEM or Coherent) coupled to a 200- μm diameter, 0.39 NA optic
426 fiber (Thorlabs) via a fiberport, and the diamond-knife cut fiber tip was placed above M1 or S1.

427 **Nerve Transection**

428 The facial nerve was transected with the mouse under isoflurane anesthesia. A small (~ 5 mm) incision,
429 centered ~ 5 - 8 mm ventral of the eye, was made in the skin. The buccal branch of the facial was
430 identified running from near the ear to the whisker pad, blunt dissected free of underlying tissue, and
431 cut. The skin was closed with stitches and bupivacaine applied.

432 **Superior Colliculus Lesion**

433 The superior colliculus was lesioned bilaterally just prior to headplate implantation. Craniotomies
434 were drilled over superior colliculus (0.5 mm anterior of lambda, 0.75 mm lateral of midline). A
435 tungsten electrode (0.3-1.0 M Ω) was inserted to depths of 1 mm and 2 mm on each side, and 300
436 μ A of current was delivered for 30 s at each lesion site. Mice were then implanted with a headplate
437 and habituated as described above. Histology was used to confirm lesion size and location, and
438 only recordings from mice with on-target lesions were analyzed.

439 **Histology**

440 At the end of experiments, mice were deeply anesthetized with sodium pentobarbital and then
441 perfused transcardially with 1X phosphate buffer followed by 4% paraformaldehyde. Brains were
442 removed and sectioned on a vibratome into 100 μ m-thick slices, or on a freezing microtome into
443 50 μ m-thick slices. 100- μ m slices were mounted directly on glass slides with mounting medium.
444 50- μ m slices were stained in a solution of Cytochrome C (0.3 mg/ml), Catalase (0.4mg/ml), and
445 3-3'-Diaminobenzidine (DAB, 0.583mg/mL). Sections were incubated in this solution at 40°C for
446 30-45 minutes. Sections were washed 5 times in 1X phosphate buffer and mounted on glass
447 slides with mounting medium.

448 **Data Analysis**

449 Putative action potentials were identified offline with custom MATLAB software. Spikes were then
450 manually sorted with MClust (version 4.3).

451 Whiskers were automatically tracked from videos using software (Clack *et al.* 2012). Custom
452 MATLAB software was used to compute the median whisker angle. The median angle was
453 bandpass filtered from 4 to 30 Hz and passed through a Hilbert transform to calculate phase. We
454 defined the upper and lower envelopes of the unfiltered median whisking angle as the points in
455 the whisk cycle where phase equaled 0 (most protracted) or π (most retracted), respectively.
456 Whisking amplitude was defined as the difference between these two envelopes. Periods of
457 whisking and quiescence were defined as times where whisking amplitude exceeded 20% of
458 maximum for at least 250 msec. Periods of time where amplitude exceeded this threshold for less
459 than 250 msec were considered ambiguous and excluded from analysis of whisking versus
460 quiescence.

461 For cross-correlation analysis, whisking angle, amplitude, pupil, and spike vectors were binned
462 with a 10-millisecond time bin. They were then normalized to have a mean of zero and standard
463 deviation of one. Cross-correlations were again normalized such that the autocorrelation at a time
464 lag of zero equaled one. To test the significance in changes between cross-correlation
465 distributions (e.g. when comparing laser-off and laser-on conditions during cortical silencing) we
466 found the lag of the peak correlation value for each distribution. We then performed paired t-tests
467 between the correlation values of each cell at that time lag.

468 For each cell, each spike that occurred while the mouse was whisking was assigned a phase.
469 The distribution of possible spike phases ($-\pi$ to π) was calculated using 32 equally sized bins.
470 Using the same binning, we then calculated the distribution of phases observed in the video to
471 determine the time the whiskers spent at various mean phases. We then normalized the spike
472 phase distribution by the phase distribution to calculate firing rate as a function of phase. The
473 modulation of the cell was characterized by fitting a sine function with a period of 2π to this rate

474 function using least-squares regression. The modulation depth was calculated as the amplitude
475 of the fitted sine wave divided by the cell's mean firing rate as in 8⁸. To test the significance of this
476 modulation, we compared the distributions of whisking phase and (unnormalized, unbinned) spike
477 phase with a Kuiper test and a Bonferroni multiple-comparisons correction.

478 Pupil diameter was measured from video using custom MATLAB software. Videos were level-
479 adjusted and thresholded to maximize the contrast between the pupil and the rest of the eye. The
480 built in `imfindcircles()` function was used to locate the pupil and measure diameter on each frame.

481

482

483 **References**

- 484 1. Phillips, J. W. *et al.* A repeated molecular architecture across thalamic pathways. *Nat. Neurosci.*
485 **22**, 1925–1935 (2019).
- 486 2. Herkenham, M. Laminar organization of thalamic projections to the rat neocortex. *Science (80-.)*.
487 **207**, 532–535 (1980).
- 488 3. Guillery, R. W. & Sherman, S. M. Thalamic Relay Functions and Their Role in Corticocortical
489 Communication: Generalizations from the Visual System. *Neuron* **33**, 163–175 (2002).
- 490 4. Chiaia, N. L., Rhoades, R. W., Bennett-Clarke, C. A., Fish, S. E. & Killackey, H. P. Thalamic
491 processing of vibrissal information in the rat. I. Afferent input to the medial ventral posterior and
492 posterior nuclei. *J. Comp. Neurol.* **314**, 201–216 (1991).
- 493 5. Sherman, S. M. & Guillery, R. W. The role of the thalamus in the flow of information to the cortex.
494 *Philos. Trans. R. Soc. London. Ser. B Biol. Sci.* **357**, 1695–1708 (2002).
- 495 6. Wimmer, V. C., Bruno, R. M., de Kock, C. P. J., Kuner, T. & Sakmann, B. Dimensions of a
496 Projection Column and Architecture of VPM and POm Axons in Rat Vibrissal Cortex. *Cereb.*
497 *Cortex* **20**, 2265–2276 (2010).
- 498 7. Constantinople, C. M. & Bruno, R. M. Deep cortical layers are activated directly by thalamus.
499 *Science (80-.)*. **340**, 1591–1594 (2013).
- 500 8. Moore, J. D., Mercer Lindsay, N., Deschênes, M. & Kleinfeld, D. Vibrissa Self-Motion and Touch
501 Are Reliably Encoded along the Same Somatosensory Pathway from Brainstem through
502 Thalamus. *PLoS Biol.* **13**, e1002253 (2015).
- 503 9. Diamond, M. E., Armstrong-James, M., Ebner, F. F., Armstrong-James, M. & Ebner, F. F. Somatic
504 sensory responses in the rostral sector of the posterior group (POm) and in the ventral posterior
505 medial nucleus (VPM) of the rat thalamus. *J. Comp. Neurol.* **318**, 462–476 (1992).
- 506 10. Moore, C. I. Frequency-Dependent Processing in the Vibrissa Sensory System. *J. Neurophysiol.*
507 **91**, 2390–2399 (2004).
- 508 11. Masri, R., Bezdudnaya, T., Trageser, J. C. & Keller, A. Encoding of stimulus frequency and sensor
509 motion in the posterior medial thalamic nucleus. *J. Neurophysiol.* **100**, 681–689 (2008).
- 510 12. Olsen, G. M. & Witter, M. P. Posterior parietal cortex of the rat: Architectural delineation and
511 thalamic differentiation. *J. Comp. Neurol.* **524**, 3774–3809 (2016).
- 512 13. Trageser, J. C. & Keller, A. Reducing the uncertainty: Gating of peripheral inputs by zona incerta.
513 *J. Neurosci.* **24**, 8911–8915 (2004).
- 514 14. Zhang, W. & Bruno, R. M. High-order thalamic inputs to primary somatosensory cortex are
515 stronger and longer lasting than cortical inputs. *Elife* **8**, (2019).
- 516 15. Mease, R. A., Metz, M. & Groh, A. Cortical Sensory Responses Are Enhanced by the Higher-
517 Order Thalamus. *Cell Rep.* **14**, 208–215 (2016).
- 518 16. Yu, C., Derdikman, D., Haidarliu, S. & Ahissar, E. Parallel Thalamic Pathways for Whisking and
519 Touch Signals in the Rat. *PLoS Biol.* **4**, (2006).
- 520 17. Urbain, N. *et al.* Whisking-Related Changes in Neuronal Firing and Membrane Potential Dynamics
521 in the Somatosensory Thalamus of Awake Mice. *Cell Rep.* **13**, 647–656 (2015).
- 522 18. Masri, R. *et al.* Zona incerta: A role in central pain. *J. Neurophysiol.* **102**, 181–191 (2009).
- 523 19. Frangeul, L. *et al.* Specific activation of the paralemniscal pathway during nociception. *Eur. J.*
524 *Neurosci.* **39**, 1455–1464 (2014).
- 525 20. Saalman, Y. B., Pinsk, M. A., Wang, L., Li, X. & Kastner, S. The pulvinar regulates information
526 transmission between cortical areas based on attention demands. *Science* **337**, 753–6 (2012).
- 527 21. Petersen, S. E., Robinson, D. L. & Morris, J. D. Contributions of the pulvinar to visual spatial
528 attention. *Neuropsychologia* **25**, 97–105 (1987).
- 529 22. Wilke, M., Turchi, J., Smith, K., Mishkin, M. & Leopold, D. A. Pulvinar inactivation disrupts
530 selection of movement plans. *J. Neurosci.* **30**, 8650–9 (2010).
- 531 23. Roth, M. M. *et al.* Thalamic nuclei convey diverse contextual information to layer 1 of visual cortex.
532 *Nat. Neurosci.* **19**, 299–307 (2016).
- 533 24. Clack, N. G. *et al.* Automated tracking of whiskers in videos of head fixed rodents. *PLoS Comput.*
534 *Biol.* **8**, e1002591 (2012).
- 535 25. Hill, D. N., Curtis, J. C., Moore, J. D. & Kleinfeld, D. Primary Motor Cortex Reports Efferent Control
536 of Vibrissa Motion on Multiple Timescales. *Neuron* **72**, 344–356 (2011).
- 537 26. Diamond, M. E., von Heimendahl, M., Knutsen, P. M., Kleinfeld, D. & Ahissar, E. ‘Where’ and
538 ‘what’ in the whisker sensorimotor system. *Nat. Rev. Neurosci.* **9**, 601–612 (2008).

- 539 27. Hong, Y. K., Lacefield, C. O., Rodgers, C. C. & Bruno, R. M. Sensation, movement and learning in
540 the absence of barrel cortex. *Nature* (2018) doi:10.1038/s41586-018-0527-y.
- 541 28. Hoogland, P. V., Welker, E. & Van der Loos, H. Organization of the projections from barrel cortex
542 to thalamus in mice studied with Phaseolus vulgaris-leucoagglutinin and HRP. *Exp. Brain Res.*
543 (1987) doi:10.1007/BF00255235.
- 544 29. Bourassa, J. & Deschênes, M. Corticothalamic projections from the primary visual cortex in rats: a
545 single fiber study using biocytin as an anterograde tracer. *Neuroscience* (1995) doi:10.1016/0306-
546 4522(95)00009-8.
- 547 30. Killackey, H. P. & Sherman, S. M. Corticothalamic projections from the rat primary somatosensory
548 cortex. *J. Neurosci.* (2003) doi:10.1523/jneurosci.23-19-07381.2003.
- 549 31. Gharaei, S., Honnuraiah, S., Arabzadeh, E. & Stuart, G. J. Superior colliculus modulates cortical
550 coding of somatosensory information. *bioRxiv* 715847 (2019) doi:10.1101/715847.
- 551 32. Berman, R. A. & Wurtz, R. H. Functional Identification of a Pulvinar Path from Superior Colliculus
552 to Cortical Area MT. *J. Neurosci.* (2010) doi:10.1523/jneurosci.6176-09.2010.
- 553 33. Castro-Alamancos, M. A. & Favero, M. Whisker-related afferents in superior colliculus. *J.*
554 *Neurophysiol.* **115**, 2265–2279 (2016).
- 555 34. Nakamura, H., Hioki, H., Furuta, T. & Kaneko, T. Different cortical projections from three
556 subdivisions of the rat lateral posterior thalamic nucleus: A single-neuron tracing study with viral
557 vectors. *Eur. J. Neurosci.* **41**, 1294–1310 (2015).
- 558 35. Guo, Z. V. *et al.* Maintenance of persistent activity in a frontal thalamocortical loop. *Nature* (2017)
559 doi:10.1038/nature22324.
- 560 36. Poulet, J. F. A. F. A. & Petersen, C. C. H. C. H. Internal brain state regulates membrane potential
561 synchrony in barrel cortex of behaving mice. *Nature* **454**, 881–885 (2008).
- 562 37. Poulet, J. F. A. F. A., Fernandez, L. M. J. M. J., Crochet, S. & Petersen, C. C. H. C. H. Thalamic
563 control of cortical states. *Nat. Neurosci.* **15**, 370–372 (2012).
- 564 38. Sherman, S. M. Thalamus plays a central role in ongoing cortical functioning. *Nat. Neurosci.* **19**,
565 533–541 (2016).
- 566 39. Pinault, D. & Deschênes, M. Projection and innervation patterns of individual thalamic reticular
567 axons in the thalamus of the adult rat: A three-dimensional, graphic, and morphometric analysis. *J.*
568 *Comp. Neurol.* **391**, 180–203 (1998).
- 569 40. Meyer, H. S. *et al.* Number and laminar distribution of neurons in a thalamocortical projection
570 column of rat vibrissal cortex. *Cereb. Cortex* **20**, 2277–2286 (2010).
- 571 41. Constantinople, C. M. & Bruno, R. M. Effects and mechanisms of wakefulness on local cortical
572 networks. *Neuron* (2011) doi:10.1016/j.neuron.2011.02.040.
- 573 42. Vinck, M., Batista-Brito, R., Knoblich, U. & Cardin, J. A. Arousal and Locomotion Make Distinct
574 Contributions to Cortical Activity Patterns and Visual Encoding. *Neuron* **86**, 740–754 (2015).
- 575 43. Reimer, J. *et al.* Pupil Fluctuations Track Fast Switching of Cortical States during Quiet
576 Wakefulness. *Neuron* **84**, 355–362 (2014).
- 577 44. Masri, R., Trageser, J. C., Bezdudnaya, T., Li, Y. & Keller, A. Cholinergic regulation of the
578 posterior medial thalamic nucleus. *J. Neurophysiol.* **96**, 2265–2273 (2006).
- 579 45. Reimer, J. *et al.* Pupil fluctuations track rapid changes in adrenergic and cholinergic activity in
580 cortex. *Nat. Commun.* **7**, (2016).
- 581 46. Varela, C. Thalamic neuromodulation and its implications for executive networks. *Frontiers in*
582 *Neural Circuits* vol. 8 (2014).
- 583 47. Petersen, S. E., Robinson, D. L. & Keys, W. Pulvinar nuclei of the behaving rhesus monkey: visual
584 responses and their modulation. *J. Neurophysiol.* **54**, 867–86 (1985).
- 585 48. Ward, R., Danziger, S., Owen, V. & Rafal, R. Deficits in spatial coding and feature binding
586 following damage to spatiotopic maps in the human pulvinar. *Nat. Neurosci.* (2002)
587 doi:10.1038/nn794.
- 588 49. Snow, J. C., Allen, H. A., Rafal, R. D. & Humphreys, G. W. Impaired attentional selection following
589 lesions to human pulvinar: evidence for homology between human and monkey. *Proc. Natl. Acad.*
590 *Sci. U. S. A.* **106**, 4054–9 (2009).
- 591 50. Karnath, H., Himmelbach, M. & Rorden, C. The subcortical anatomy of human spatial neglect:
592 putamen, caudate nucleus and pulvinar. *Brain* **125**, 350–360 (2002).
- 593 51. Musall, S., Kaufman, M. T., Juavinett, A. L., Gluf, S. & Churchland, A. K. Single-trial neural
594 dynamics are dominated by richly varied movements. *Nat. Neurosci.* **22**, 1677–1686 (2019).

- 595 52. Reinhold, K., Lien, A. D. & Scanziani, M. Distinct recurrent versus afferent dynamics in cortical
596 visual processing. *Nat. Neurosci.* (2015) doi:10.1038/nn.4153.
- 597 53. Gambino, F. *et al.* Sensory-evoked LTP driven by dendritic plateau potentials in vivo. *Nature* **515**,
598 116–119 (2014).
- 599 54. Williams, L. E. & Holtmaat, A. Higher-Order Thalamocortical Inputs Gate Synaptic Long-Term
600 Potentiation via Disinhibition. *Neuron* **101**, 91-102.e4 (2019).
- 601 55. Audette, N. J., Bernhard, S. M., Ray, A., Stewart, L. T. & Barth, A. L. Rapid Plasticity of Higher-
602 Order Thalamocortical Inputs during Sensory Learning. *Neuron* **103**, 277-291.e4 (2019).
- 603 56. Heaton, J. T. *et al.* Rat whisker movement after facial nerve lesion: Evidence for autonomic
604 contraction of skeletal muscle. *Neuroscience* (2014) doi:10.1016/j.neuroscience.2014.01.038.
- 605 57. Paxinos, G. & Franklin, K. B. J. *Paxinos and Franklin's The Mouse Brain in Stereotaxic*
606 *Coordinates*. (Elsevier Inc., 2019).
- 607

Figure 1: POm cells mainly track slow components of whisking activity

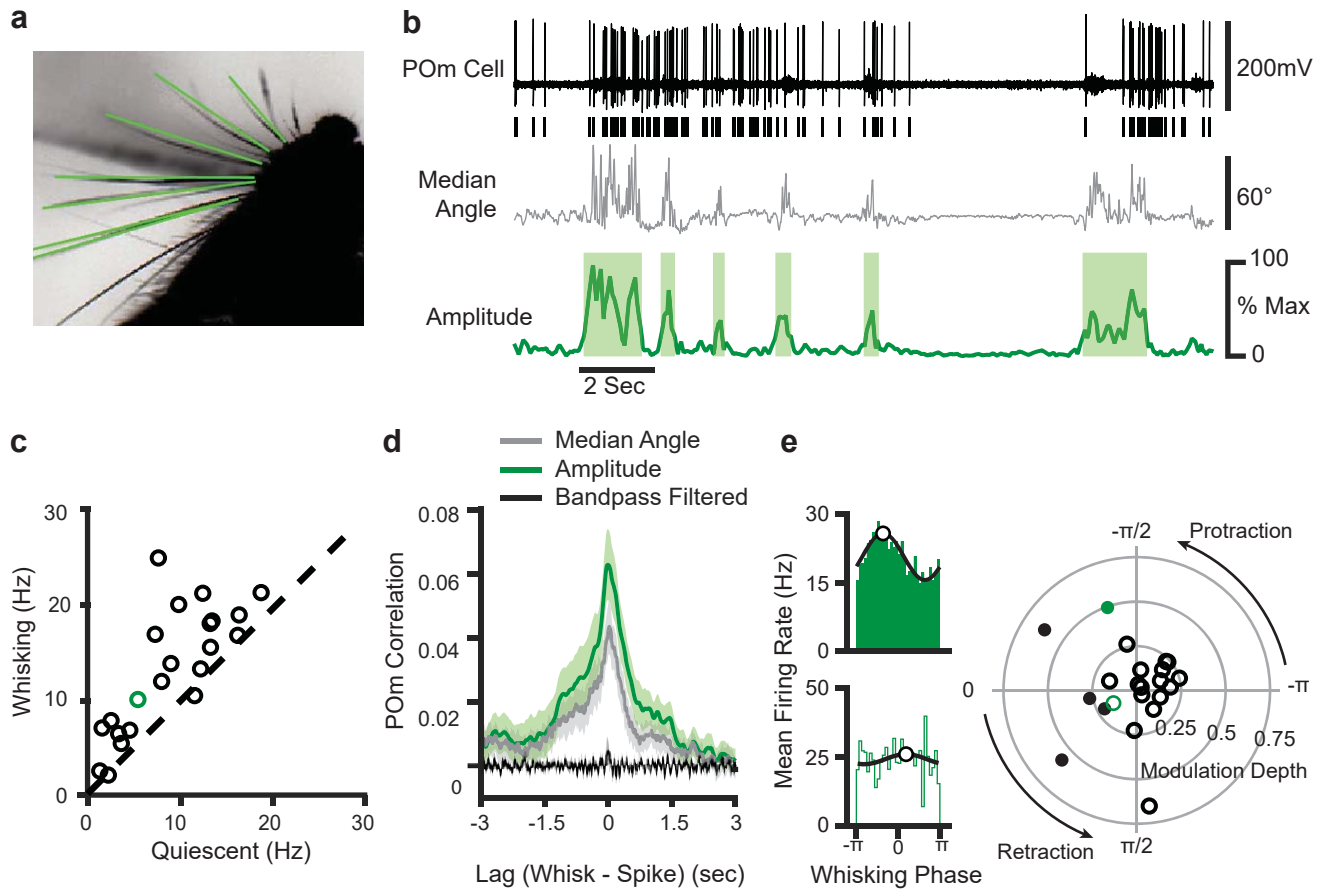


Figure 2: POm encodes whisking in absence of refferent sensory input.

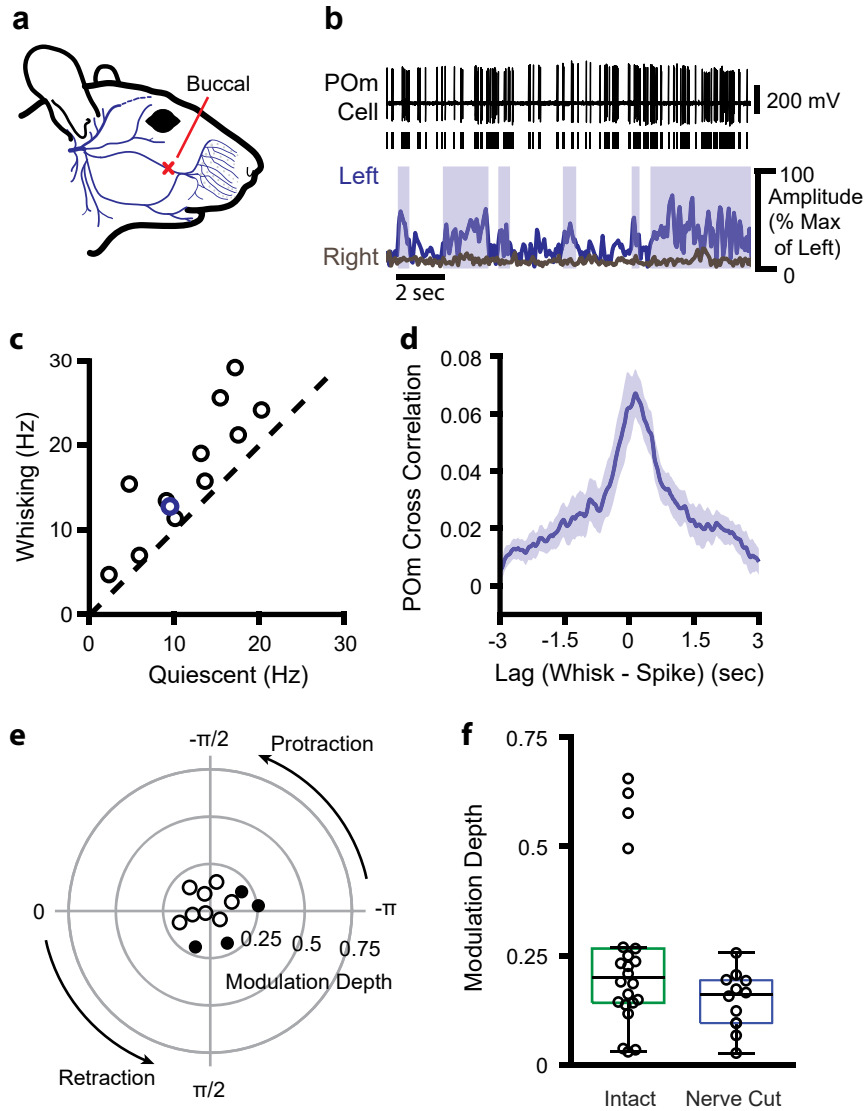


Figure 3: Inhibition of primary motor cortex increases POm correlation with whisking

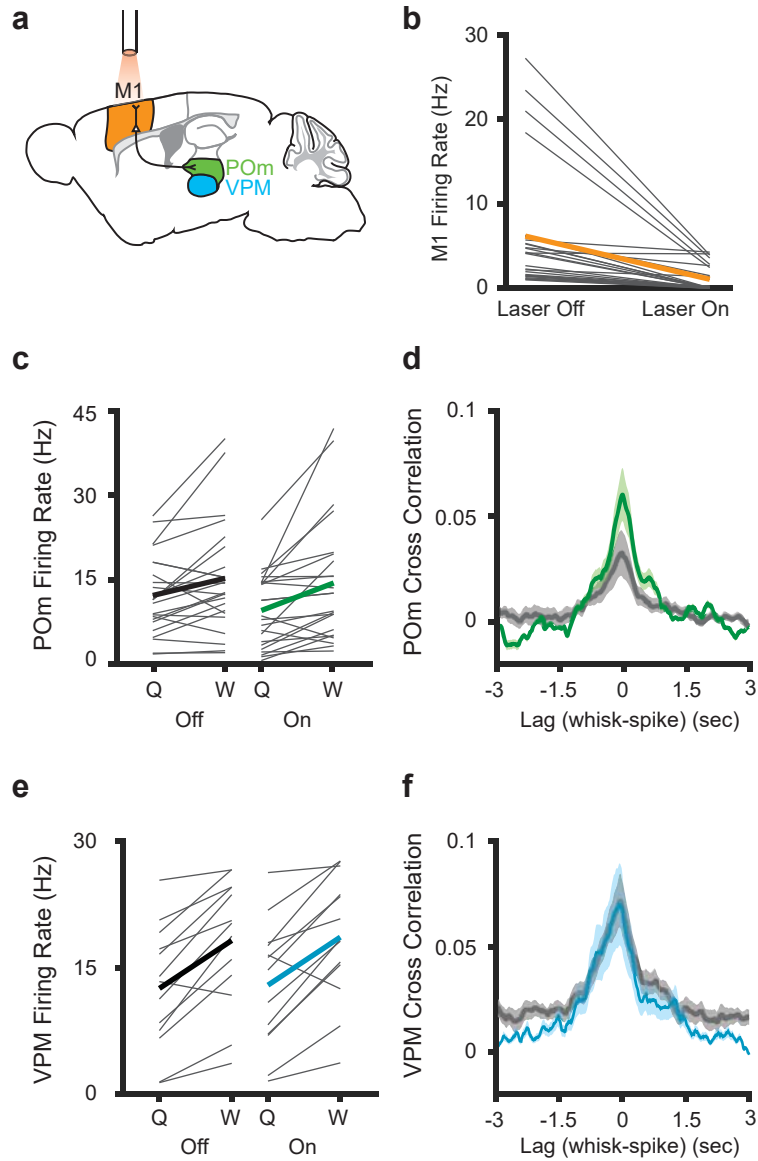


Figure 4: Inhibition of primary somatosensory cortex increases POm correlation with whisking.

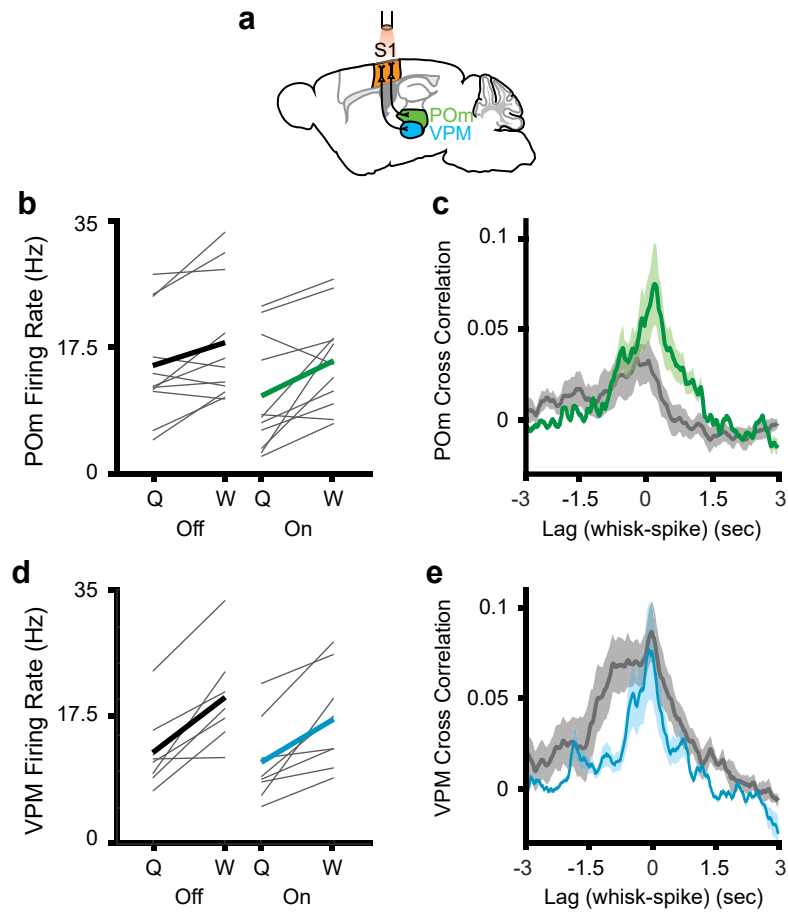


Figure 5: Lesion of Superior Colliculus does not reduce correlation of POm activity and whisking

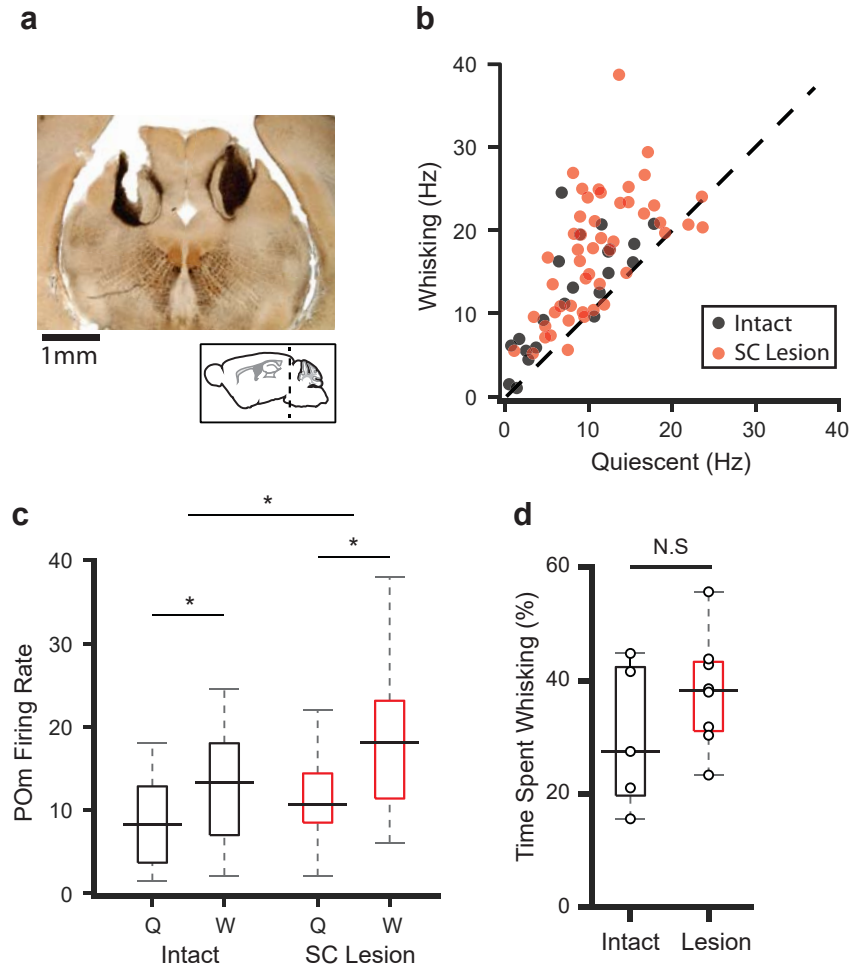


Figure 6: POm activity tracks pupil dynamics

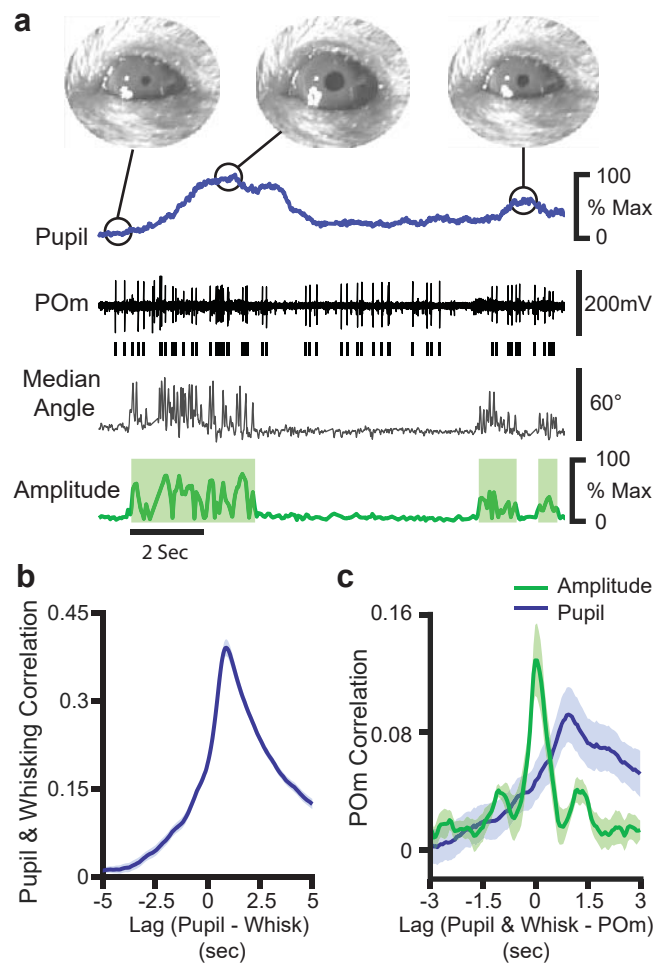


Figure 7: LP activity tracks slow whisker dynamics.

